GRACE-Based Estimates of Terrestrial Freshwater Discharge from Basin to Continental Scales

TAJDARUL H. SYED AND JAMES S. FAMIGLIETTI

Department of Earth System Science, University of California, Irvine, Irvine, California

DON P. CHAMBERS

Center for Space Research, University of Texas, Austin, Texas

(Manuscript received 14 November 2007, in final form 18 April 2008)

ABSTRACT

In this study, new estimates of monthly freshwater discharge from continents, drainage regions, and global land for the period of 2003–05 are presented. The method uses observed terrestrial water storage change estimates from the Gravity Recovery and Climate Experiment (GRACE) and reanalysis-based atmospheric moisture divergence and precipitable water tendency in a coupled land–atmosphere water mass balance. The estimates of freshwater discharge are analyzed within the context of global climate and compared with previously published estimates. Annual cycles of observed streamflow exhibit stronger correlations with the computed discharge compared to those with precipitation minus evapotranspiration ($P - E$) in several of the world's largest river basins. The estimate presented herein of the mean monthly discharge from South America ($\sim$846 km^3 month^{-1}) is the highest among the continents and that flowing into the Atlantic Ocean ($\sim$1382 km^3 month^{-1}) is the highest among the drainage regions. The volume of global freshwater discharge estimated here is 30 354 $\pm$ 1212 km^3 yr^{-1}. Monthly variations of global freshwater discharge peak between August and September and reach a minimum in February. Global freshwater discharge is also computed using a global ocean–atmosphere mass balance in order to validate the land–atmosphere water balance estimates and as a measure of global water budget closure. Results show close proximity between the two estimates of global discharge at monthly (RMSE = 329 km^3 month^{-1}) and annual time scales (358 km^3 yr^{-1}). Results and comparisons to observations indicate that the method shows important potential for global-scale monitoring of combined surface water and submarine groundwater discharge at near–real time, as well as for contributing to contemporary global water balance studies and for constraining global hydrologic model simulations.

1. Introduction

As a key component of the water cycle, freshwater discharge integrates a host of physical and biogeochemical processes crucial for sustaining ecosystems, influencing climate and related global change. The hydrologic consequences of changes in global climate have become a major concern for scientists and policymakers alike. As such, it has become increasingly clear that pragmatic, real-time information on freshwater water discharge, at varied spatial scales and over the globe, is of paramount importance in assessing changes in the earth system. However, integrated global networks of such observations are plagued by numerous technical, political, and economic challenges. Currently, there exists no comprehensive global network for the monitoring of freshwater discharge into the world oceans (Alsdorf and Lettenmaier 2003; Brakenridge et al. 2005). To date, the majority of the reported assessments of global discharge are either based on modeled runoff, climatologies of precipitation minus evaporation ($P - E$), or on gauge-based observations, made over varying time periods (some in the distant past) and having variable accuracies. Moreover, even gauge-based observations require either model simulations or $P - E$ as a proxy for discharge to quantify contributions from ungauged regions. The problem is further compounded by a strong dissuasion for data sharing (Rodda et al. 1993) and a worldwide decrease in the density of

Corresponding author address: James S. Famiglietti, Dept. of Earth System Science, University of California, Irvine, Irvine, CA 92697.
E-mail: jfamigli@uci.edu

DOI: 10.1175/2008JHM993.1

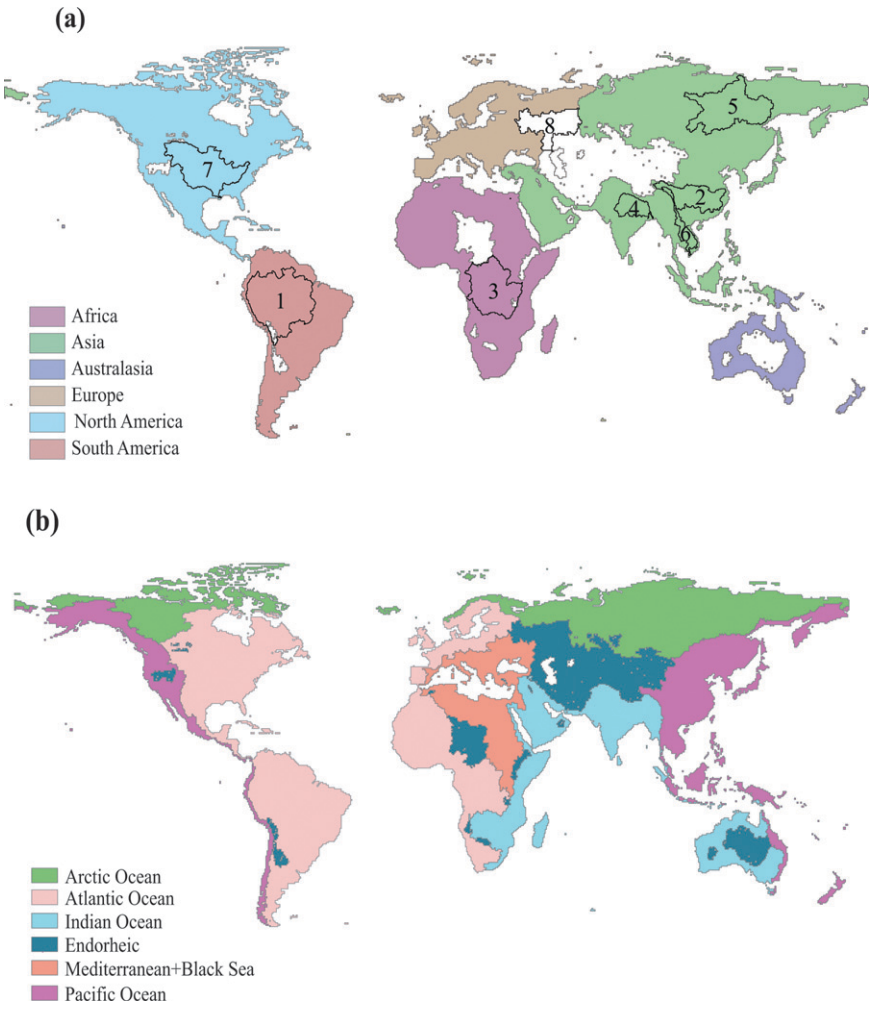

FIG. 1. (a) Map of the exorheic portions of each continent excluding Greenland and Antarctica. Also shown are some of some of the world's largest river basins: 1) Amazon, 2) Chang Jiang, 3) Congo, 4) Ganges, 5) Lena, 6) Mekong, 7) Mississippi, and (8) Volga. (b) Map of the drainage regions, excluding Greenland and Antarctica, contributing to flows into the world oceans. Adapted from STN-30p (Vörösmarty et al. 2000a).

hydrologic monitoring stations (Stokstad 1999; Shikomanov et al. 2002). Thus, missing or even delayed information on global freshwater discharge from the recent past inhibits any consistent evaluation of global, terrestrial freshwater discharge for the current era.

In this study, we present large-scale, monthly estimates of freshwater discharge using Gravity Recovery and Climate Experiment (GRACE) derived monthly terrestrial water storage changes in a combined land–atmosphere water mass balance, for the 3-yr period from 2003 to 2005. Terrestrial water storage consists of all forms of water stored above and underneath the land surface, including snow, surface waters, soil moisture, and groundwater. The current investigation expands upon the previous work of Syed et al. (2005, 2007) that used the same methodology to estimate the total basin discharge for the Amazon and Mississippi River basins and for the pan-Arctic drainage region. Here, we significantly expand upon the previous work to estimate freshwater discharge for several large river basins, the continents (Fig. 1a), drainage regions (Fig. 1b), 10° latitudinal zones, and for all global land. Further, we comprehensively compare our estimates to those from other studies, and we also assess global water budget closure at monthly and seasonal time scales by comparing global land and ocean water balances.

The primary objective of this study is to present and analyze gauge-independent, observation-based estimates of terrestrial freshwater discharge into the ocean. Implicit in our mass balance estimates and discussed

with greater detail later in this paper is the inclusion of flows from ungauged portions of contributing drainage regions, braided stream channels, and direct groundwater flows. In contrast to previous studies, our estimates of global and continental discharges represent the net of surface and groundwater flows (Syed et al. 2005), are made at monthly intervals and in near–real time, and they do not include contributions from the large internally draining regions of the globe. Furthermore, the availability of terrestrial water storage change information from GRACE allows us to relax the assumption that this term is on annual average equal to zero, as in the case of prior $P - E$ based discharge estimates (Oki et al. 1995; Oki 1999; Dai and Trenberth 2002). Therefore, freshwater discharge estimated in this study has potential applications for a variety of hydrologic and climate-related studies including global mean sea level rise and water resources assessment.

While the current methodology enables the characterization of terrestrial freshwater outflows across varied temporal (monthly and longer) and spatial scales [$>200\ 000\ km^2$, the lower limit of GRACE water storage detectability; Rodell and Famiglietti (1999)], it cannot resolve important features of the distribution of terrestrial surface waters at higher spatiotemporal frequencies (i.e., heights, slopes, inundation extent, and storage changes in lakes, reservoirs, rivers, wetlands, and floodplains). This higher-resolution information on surface water dynamics will be best captured by a hydrology-specific altimetry mission (Alsdorf et al. 2007; NRC 2007). The method that we present here, when combined with information from a potential dedicated surface water mission, will provide a complete picture of the flow of terrestrial waters over and through large river basins and continental regions.

2. Background

a. Global freshwater discharge

Since the pioneering work by Baumgartner and Reichel (1975), there have been a myriad of studies aimed at the estimation of continental and global freshwater discharge. The majority of these studies reported discharges based on any or a combination of the following: (a) in situ gauge-based streamflow (Perry et al. 1996; Shiklomanov 2003), (b) model simulations of runoff (Nijssen et al. 2001), and (c) precipitation minus evaporation (Baumgartner and Reichel 1975; Oki et al. 1995; Oki 1999; Schlosser and Houser 2007). A brief review of these methods is presented below.

In situ measurement of streamflow, notwithstanding its limitations, has been the primary source of knowledge on surface water dynamics and a longstanding measure of hydrologic model performance. While often used as a surrogate for net outflow in basin-scale water balance studies (Gutowski et al. 1997; Seneviratne et al. 2004; Betts et al. 2005), in-channel streamflow measured at the gauging stations may in reality represent only a part of the net freshwater flux and is therefore incomplete for comprehensive budget analyses (Oki et al. 1995; Alsdorf and Lettenmaier 2003; Syed et al. 2005). Large-scale flow diversification in deltaic regions, floodplain inundation, direct groundwater flows [estimated to be ~10% of global runoff; Zektser and Loaiciga (1993)], and drainage into wetlands [composed of ~4% of the global land area; Prigent et al. (2001)] are some of the many pathways of basin water outflow that are not registered by conventional stream gauges.

Gauge-based estimates of global and continental freshwater discharge are limited by geographic and political restrictions due to institutional and economic constraints. Existing regional networks are often located in affluent portions of the world. Quantification of freshwater discharge into the ocean is further complicated by the fact that existing stream gauges are often located long distances from the point of inflow into the ocean (Dai and Trenberth 2002). Less than 60% of the global distribution of in situ stream gauges is located near mouths of rivers (Bjerklie et al. 2003). Upstream flow estimates are usually, but not always, lower than those measured farther downstream. Further, global estimates of freshwater discharge into the world oceans based on upscaling of climatologic discharge from selected river basins may over- or underestimate the true global value.

Apparent differences in the reported annual estimates of global discharge, including those purely based on observations (Probst and Tardy 1987; Perry et al. 1996; Shiklomanov 2003), can be attributed to a variety of sources. Differences in the number of rivers selected, length of time considered, interpolation techniques used to fill in gaps in the datasets, and the consideration of flows from ungauged portions are some of the major causes behind the noted discrepancies.

In spite of the major advances in land surface models and data assimilation techniques, there remain large discrepancies between observations and model simulations of discharge. Primary drawbacks in current global land surface models are limitations in accounting for human-induced effects on the hydrologic cycle (Haddeland et al. 2006) and the poor representation of wetlands and floodplains (Coe 2000). In an assessment of

the water budget over the Mississippi River basin, Roads et al. (2003) found modeled runoff and observed discharge differ by ~50%. In another study by Coe (2000), simulated mean annual discharge from a global hydrologic model was found to be within ~20% of the observed discharge at only 13 of 90 gauging stations used for the comparison. Similarly, a model intercomparison study (Lohmann et al. 2004) reported that regional differences in mean annual runoff roughly vary by a factor of 4.

Some recent studies have synthesized modeled and observed data to compensate for some of the abovementioned deficiencies. Fekete et al. (2000, 2002) used observed discharge data from the Global Runoff Data Center (GRDC; information online at http://grdc.bafg.de) to constrain modeled estimates of runoff. The data-merging approach was furthered improved by Dai and Trenberth (2002), for flows into world oceans, by incorporating a river-routing scheme (Branstetter 2001) to transport the runoff to appropriate ocean-draining model grids.

Alternatively, at interannual time scales, net precipitation over land ($P - E$) has been used as a proxy for runoff in the majority of prior studies, based on the common assumption of negligible storage changes. While some of the reported studies are based on hydrologic model simulations of E and observations of P (Baumgartner and Reichel 1975; Schlosser and Houser 2007), others are based on atmospheric moisture balance computations using a global analysis of column-integrated atmospheric moisture divergence (Oki et al. 1995; Oki 1999; Dai and Trenberth 2002). Although hindered by the assumption of zero storage change (Oki 1999; Dai and Trenberth 2002), estimates of discharge from the atmospheric moisture budget proved to be better than those purely based on model simulations (Dai and Trenberth 2002).

The present study complements those mentioned above. While addressing several of the aforementioned shortcomings, including accounting for terrestrial water storage changes using GRACE, the current work presents the estimation of a holistic value of total discharge that includes all surface and groundwater flows, and that can be applied at varied spatial scales and at monthly intervals.

b. GRACE: Terrestrial water storage changes

GRACE is a joint satellite mission between the National Aeronautics and Space Administration (NASA) and the German space agency Deutsches Zentrum für Luft- und Raumfahrt (DLR), and was launched in March 2002 (Tapley et al. 2004). The mission's primary objective is to provide highly accurate maps of Earth's static and time-varying gravity fields; over land, month-to-month variations of Earth's gravity field have been largely attributed to water mass movement in the land surface hydrologic cycle (Wahr et al. 1998, 2004).

Thus, for the first time, the GRACE mission is providing satellite-based, global observations of terrestrial water storage variations at monthly intervals and at spatial scales ranging from large river basins (>200 000 km^2) (Swenson et al. 2003; Chen et al. 2005; Seo et al. 2006) to continents (Ramillien et al. 2005; Schmidt et al. 2006; Syed et al. 2008).

Recent assessments of GRACE-derived water storage variations have shown good agreement with global land surface hydrological models and observations (Frappart et al. 2006; Niu and Yang 2006; Swenson et al. 2006; Swenson and Milly 2006; Syed et al. 2008). Furthermore, monthly changes in terrestrial water storage derived from GRACE have allowed for the estimation of important hydrologic fluxes including evapotranspiration (Rodell et al. 2004; Ramillien et al. 2006a), discharge (Syed et al. 2005, 2007), $P - E$ (Swenson and Wahr 2006a), groundwater storage changes (Rodell et al. 2007, Yeh et al. 2006; Swenson et al. 2007), and more importantly for the closure of the water balance at multiple scales. To date, most previous water balance studies (Oki et al. 1995; Dai and Trenberth 2002; Seneviratne et al. 2004) were forced to assume zero year-to-year variation of land water storage, primarily due to the lack of storage change observations in spatial and temporal scales relevant to such studies. Thus, GRACE's capabilities to monitor land water storage at monthly intervals, over large river basins, represent a major advance toward understanding the role of storage in basin- and larger-scale hydrologic budgets.

This study uses recent releases (RL) of GRACE data from two of the three relevant science data centers: the GeoForschungs Zentrum (GFZ) RL03 and the Jet Propulsion Laboratory (JPL) RL03. These datasets span from February 2003 to August 2006 with the exception of June 2003 and January 2004. The coupled land–atmosphere water balance, described below, requires observations or estimates of atmospheric moisture storage and divergence. We take these from two available global reanalysis products: one from the National Centers for Environmental Protection–National Center for Atmospheric Research (NCEP–NCAR; Kalnay et al. 1996) and the other from the European Centre for Medium-Range Forecasts (ECMWF) operational forecast analysis (information online at http://www.ecmwf.int/research/ifsdocs/CY25rl/index.html and http://www.ecmwf.int/products-/data/operational_system/evolution/index.html). The length of the currently available re-

analysis datasets, until December 2005 for NCEP–NCAR and May 2005 for ECMWF, restricted this study to the use of consecutive months of GRACE data through December 2005, 30 months in total. Therefore, ECMWF-based discharge estimates have a shorter span (23 months) in comparison to those based on NCEP–NCAR (30 months).

Smoothing of monthly gravity fields, in order to reduce spatial noise from the short-wavelength spherical harmonic coefficients, is a necessary step in the processing of GRACE data. Although numerous smoothing techniques have been demonstrated (Wahr et al. 1998; Han et al. 2005; Rowlands et al. 2005; Seo and Wilson 2005), for this study we use a Gaussian averaging kernel with a half-width of 400 km. Note that, depending on the length of the Gaussian filter (half width) used, portions of the signal may be suppressed along with the noise (Chen et al. 2006a). While a larger half-width can reduce the amplitude of the storage change signal, a smaller half-width can significantly decrease the signal-to-noise ratio and may even produce nongeophysical north–south stripes (Swenson and Wahr 2006b). To make an accurate quantification of GRACE-based water storage variations, we investigated the potential impacts of smoothing and postprocessing at the spatial scales used in this study. Using synthetic hydrology data, we have analyzed the effects of smoothing and postprocessing removal of correlated errors (Swenson and Wahr 2006b) by performing a regression analysis on the actual–nonsmoothed and smoothed–destriped data. Results (not shown here) demonstrated that for each of the continents, drainage regions, and for global land, there was negligible reduction in signal strength. Consequently, the scale factors (Velicogna and Wahr 2006a,b) required to restore the signal strength, determined by the slope of the best-fit line, were on average equal to one.

The accuracy of water storage change estimates observed by GRACE ranges from 1.5 cm to less than a millimeter depending on the geographic domain over which the data are averaged (Wahr et al. 2004; Ramillien et al. 2006a). In general, errors in GRACE data are representative of a combination of instrument and processing errors, which include truncation errors, leakage errors due to contaminating signals from neighboring regions, and separation errors due to the inexact removal of mass variations in the atmospheric column and in the solid earth below. Importantly, GRACE data used here employ all of the latest improvements in data processing, particularly the use of a new mean gravity field model, an ocean pole tide model, and a new ocean tide model (Chambers 2006). In addition, these datasets incorporate a postprocessing procedure to remove certain systematic errors that improves the accuracy of GRACE data at smaller spatial scales (Chambers 2006).

3. Estimation of terrestrial freshwater discharge

Effective over large spatial scales ($>10^5$ km^2) and at monthly or longer time periods, the basic concept of land–atmosphere water balance circumvents the use of less-constrained terrestrial hydrologic fluxes like evapotranspiration in land-only water balance estimates of discharge [see Eq. (1) below]. While precipitation is extensively monitored, evapotranspiration remains far more difficult to measure and quantify and is therefore limited by large uncertainties. Here, we present a brief overview of the combined land–atmosphere water balance. For a detailed discussion of the method, see Peixóto and Oort (1992) and references therein.

Over large areas, the column-integrated terrestrial water (including surface and groundwater) budget is given by the following equation:

$$\frac{\partial S}{\partial t} = P - E - R_l, \tag{1}$$

where S represent all forms of land water storage observed by GRACE, P is precipitation, E is evapotranspiration, and R_l is terrestrial freshwater discharge. In this work, ∂t is approximately 30 days, consistent with the temporal sampling of GRACE data. Here, R_l, represents the total of surface and groundwater outflows [i.e., total basin discharge; Syed et al. (2005)].

The atmospheric moisture budget can be formalized as follows:

$$\frac{\partial W}{\partial t} = E - P - \nabla \cdot \mathbf{Q}, \tag{2}$$

$$W = \int_{pT}^{pS} q \frac{dp}{g}, \tag{3}$$

$$\mathbf{Q} = \int_{pT}^{pS} q\mathbf{V} \frac{dp}{g} \quad \text{and} \tag{4},$$

$$P - E = -\frac{\partial W}{\partial t} - \nabla \cdot \mathbf{Q}, \tag{5}$$

where W is the total column water vapor and $\nabla \cdot \mathbf{Q}$ is the horizontal divergence of the vertically integrated vapor flux; P_T and P_S are pressures at the top of the atmosphere and on the surface, respectively; q is the specific humidity; g is the gravitational acceleration; and $\mathbf{V}$ is the horizontal wind velocity. In this study, the divergence and precipitable water terms in Eq. (2) were

computed from the NCEP–NCAR and ECMWF datasets. Reanalysis procedures employ four-dimensional data assimilation techniques to incorporate a variety of observed and satellite data into from numerical weather prediction models. Although not totally free from limitations (Cullather et al. 2000), reanalysis data provide an important contribution to the assessment of global and terrestrial hydrologic budgets (Oki et al. 1995; Dai and Trenberth 2002). Note that the combination of atmospheric moisture budget terms in Eq. (5) ($-\partial W/\partial t - \nabla \cdot \mathbf{Q}$) has been frequently used as an alternative to $P - E$ in global- and regional-scale water budget studies (Trenberth and Guillemot 1998; Oki 1999; Trenberth et al. 2007). Following the same convention, $P - E$ has been used and referred to in this study interchangeably with the atmospheric moisture budget terms ($-\partial W/\partial t - \nabla \cdot \mathbf{Q}$).

Estimates of freshwater discharge are computed by combining (1) and (2), referred to here as the combined land–atmosphere water balance equation. The land–atmosphere water balance equation, solving for R_l, is given by

$$R_l = -\frac{\partial S}{\partial t} - \frac{\partial W}{\partial t} - \nabla \cdot \mathbf{Q}. \quad (6)$$

Because terrestrial water storage change estimates from GRACE are changes in storage averaged over a period of ~30 days, additional care is required to aggregate the hydrologic fluxes in (6). In this study, these fluxes are aggregated following the scheme described in Syed et al. (2005). Because GRACE-derived storage changes have nominally occurred between the 15th day of each month, compatible estimates of $\nabla \cdot \mathbf{Q}$ were computed by integrating daily basin averages between the 15th day of consecutive months and that of $\partial W/\partial t$ by taking the differences between the 15th-day averages of one month from that of the following. Although alternative methods of aggregation have been published (Rodell et al. 2004; Swenson and Wahr 2006a), comparisons with the current method produced no discernible difference in the estimates of total freshwater discharge.

While our water balance–based discharge estimates compensate for some of the noted deficiencies in gauge-based discharge, they are affected by errors in the terms on the right-hand side of (6). In addition to the brief discussion presented earlier, the reader is referred to Swenson et al. (2003) and Wahr et al. (2006) for a detailed review of the quantification and sources of error in GRACE data. The precipitable water tendency term in the reorganized atmospheric moisture budget Eq. (5) contributes the least toward the magnitude and uncertainties in monthly $P - E$ estimates. On the contrary, $\nabla \cdot \mathbf{Q}$ appears as a leading term (Roads et al. 2003; Seneviratne et al. 2004) and also contributes significantly toward the errors in $P - E$ estimates obtained from the atmospheric moisture budget (5). Errors in $\nabla \cdot \mathbf{Q}$ can be attributed to several computational and observational sources. Most noted among these sources are precipitation biases, interpolation schemes, orographic effects, and errors in wind data and in the use of analysis forcings (nudging) (Roads and Betts 2000). As a result, the reorganized moisture budget Eq. (5) occasionally yields unusually large, negative values of $P - E$ that can result in negative discharge. Although it is physically possible to obtain negative discharge (e.g., in areas with significant seawater intrusion or during storm surges), they are unrealistic at the larger spatial and temporal scales considered here.

For the months in which $P - E$ estimates, integrated over continents and drainage regions (Figs. 1a and 1b) are negative, we replace the value of $P - E$ with that of an area-integrated storage change observed by GRACE, thereby making our estimated discharge equal to zero for that particular month. Essentially, we are assuming that even though it is possible to have negative $P - E$ at very localized scales, due to high evaporation rates (e.g., over irrigated fields, reservoirs, and lakes), at continental scales, negative $P - E$ can only be due to errors in the reanalysis models or in the data that are being assimilated. Thus, instead of resetting negative $P - E$ values to zero on a grid-by-grid basis (Dai and Trenberth 2002), which can lead to the major overestimation of runoff, we correct their areal integrations.

Uncertainties in our discharge estimates are computed at a 95% confidence level using the statistical propagation of errors through (6). The root-mean square (RMS) of the residuals from the least square fit, consisting of annual, semiannual, and linear terms, is used as a conservative estimate of the upper bound of error in water storage changes observed by GRACE (Wahr et al. 2006). Errors in the atmospheric moisture terms from reanalysis were assumed to be 10% due to the lack of any known published estimates. Larger errors in these terms would result in larger uncertainties of our discharge estimates.

4. Climatological discharge comparison at river basin scales

Almost all recent assessments of global discharge have been restricted to long-term annual means, which is primarily a reflection of the limited availability of

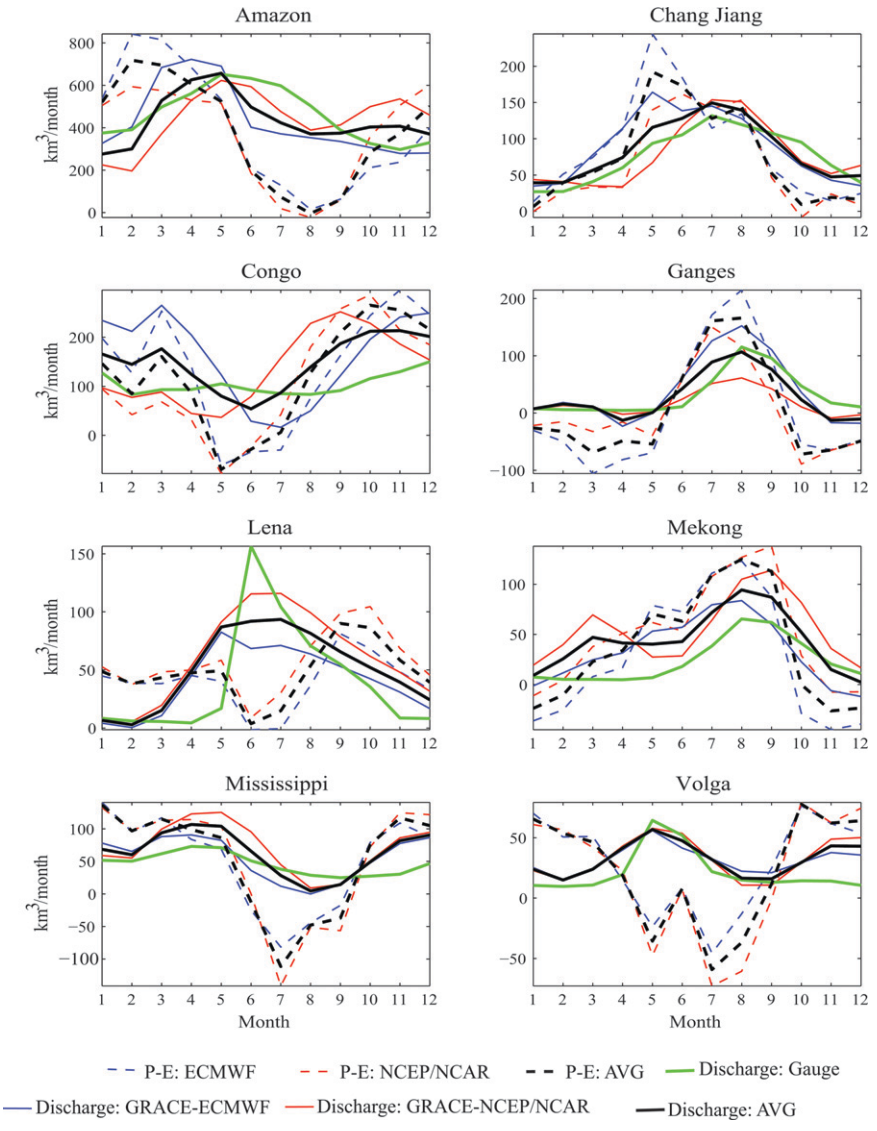

FIG. 2. Comparison of the annual cycles of estimated discharge with those of $P - E$ and observed streamflow in some of the world's largest river basins.

recent gauge-based observations. Although we later present monthly discharge time series for 2003–05, we first compare annual cycles of climatologic river discharge observed at gauging stations with those of estimated discharge and $P - E$ derived from (5) using the NCEP–NCAR and ECMWF reanalyses for the same time period. Gauge data were acquired from the GRDC for the following river basins: Amazon, Chang Jiang, Congo, Ganges, Lena, Mekong, Mississippi, and Volga (Fig. 1a). Due to the lack of gauge-based streamflow data over the study period, annual cycles of the observed discharge were computed using data over varying periods of time since the mid–twentieth century. These are compared to the annual cycle of our GRACE-based estimates for the 2003–05 time period.

Figure 2 shows the annual cycles of the observed discharge (solid green line) with those of the estimated discharge [solid lines in blue (GRACE–ECMWF), red (GRACE–NCEP–NCAR), and black (the average of GRACE–NCEP–NCAR and GRACE–ECMWF)] and $P - E$ [broken lines in blue (ECMWF), red (NCEP–NCAR), and black (the average of NCEP–NCAR and ECMWF)]. The overall agreement between the observed streamflow and estimated discharge is better than that with $P - E$. The correlations between the observed and estimated discharges range from a high of 0.92 in Chang Jiang to a low of 0.56 in Congo. In

comparison, correlations between observed streamflow and $P - E$ ranged from -0.52 (in the Volga) to 0.73 (in the Ganges). Therefore, in almost every basin, the inclusion of GRACE-derived $\partial S/\partial t$ in (6) leads to a better representation of the annual cycle of the freshwater discharge. In contrast to those results obtained from the observed streamflow, the annual cycles of the GRACE-based discharge are computed over the 2003–05 time period only and can in part explain some of the noted discrepancies. Additionally, the discharge computed using the average of GRACE–ECMWF and GRACE–NCEP–NCAR ($R \approx 0.78$; $p < 0.05$) shows improved correlation with the observed discharge when compared to those computed using ECMWF ($R \approx 0.67$; $p < 0.05$) and NCEP–NCAR ($R \approx 0.66$; $p < 0.05$) based $P - E$ estimates separately. We believe that the averaging of the GRACE–ECMWF and GRACE–NCEP–NCAR estimates negates some of the intermodel differences in the reanalysis products to provide a robust estimate of the terrestrial freshwater discharge (Syed et al. 2007).

In the Congo River basin, large discrepancies are noted between the GRACE–ECMWF and GRACE–NCEP–NCAR discharge estimates, although their average compared well with the observed gauge discharges. At the same time, the annual cycles of the $P - E$ estimates showed minor agreement with the observed discharge, both in terms of the amplitude and phase of the variability. Significant inconsistencies are also noted in the Amazon and Mississippi River basins. A characteristic difference in the annual cycles of the $P - E$ and the observed streamflow is observed across the latitudes. While $P - E$ estimates are positively correlated with observed streamflow in most of the low-latitude basins (in Fig. 2), strong anticorrelations are seen with peak discharges in the high-latitude [Lena ($R = -0.48$) and Volga ($R = -0.52$)] river basins. This phenomenon is a reflection of the fact that the peak discharges in these basins are mostly driven by changes in storage and not the excess of evapotranspiration. It is therefore evident that despite the corrections, that is, resetting of negative $P - E$ values to zero (Dai and Trenberth 2002), the approximation of $P - E$ as a surrogate for the discharge may not be applicable in the high-latitude river basins.

5. Continental freshwater discharge

Month-to-month variations in freshwater discharge are shown in Fig. 3 for each of the continents excluding Antarctica. Results shown are the average of GRACE–ECMWF and GRACE–NCEP–NCAR discharge estimates for the common period (i.e., March 2003–May 2005). The triangles in Fig. 3 represent the actual monthly values, while the solid lines show the fitted seasonal cycles (least squares fit of annual, semiannual, and linear terms). Note that different scales are used to emphasize the variations in amplitude of the seasonal cycles. In contrast to most previous global discharge studies, the current estimates are obtained exclusively from the exorheic (i.e., those that drain to the oceans) portions of each continent defined in simulated topological network at 30′ latitude × longitude spatial resolution (STN-30p; Vörosmarty et al. 2000a). Globally, endorheic (i.e., internally draining) regions account for about 13% of the nonglaciated global landmass. The relative importance of endorheic regions varies depending on the continent. Continental North and South America are mostly connected to the oceans, whereas ~28% of Australasia and ~20% of Asia are internally draining.

The mean monthly discharge (i.e., the average discharge per month from the average of GRACE–ECMWF and GRACE–NCEP–NCAR estimates for the study period, also shown as the broken line in Fig. 3) from South America is the largest (~846 km^3 $month^{-1}$) among all the continents followed by that from Asia (~619 km^3 $month^{-1}$) and then North America (~539 km^3 $month^{-1}$) (see Table 1 for details). Freshwater discharge peaks in April for South America, in August–September for Asia and North America, in February for Europe and Australasia, and in November for Africa. Amplitudes of variability range between 639.2 km^3 $month^{-1}$ from Asia and 42 km^3 $month^{-1}$ from Australasia (Table 1).

The overall timing and magnitude of the peaks in fitted seasonal cycles of discharge are coincident with the seasonal shifts in the intertropical convergence zone (ITCZ) and, more generally, with the amount of precipitation. The highly periodic influence of snowmelt in the Northern Hemisphere high latitudes, and heavy precipitation in the tropics due to the Indian and Southeast Asian monsoons, is clearly reflected in the timing and highest amplitude of the variability in the discharge from Asia. In contrast Australasia is a predominantly dry continent and therefore generates the least amount of discharge into the ocean. Illustrated in Fig. 3b are the relative contributions of each continent toward the global freshwater discharge in terms of annual mean and the percentage of the total. Outflows from South America clearly dominate the annual terrestrial discharge with a contribution of about 34% of the annual global mean, followed closely by that from Asia (25%) and North America (~22%). These three continents combined contribute to about 80% of the freshwater flowing into the global oceans.

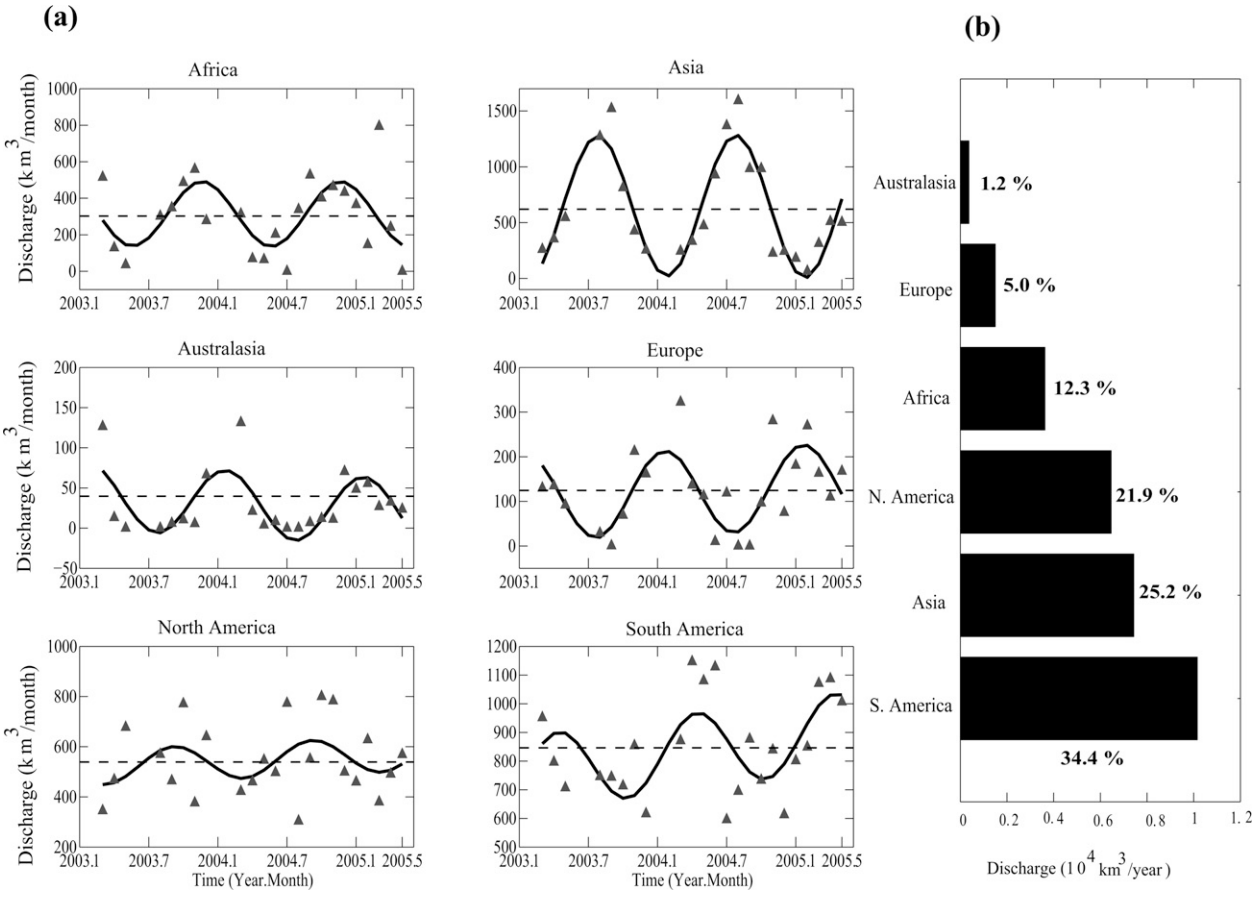

FIG. 3. (a) Monthly variations of freshwater discharge from individual continents (triangles) and their fitted seasonal cycles (solid black line). The mean monthly discharge for the study period is shown as broken black lines. (b) Relative contributions of freshwater discharge from each continent expressed as a percentage of the global discharge.

In Table 2 we place our study within the context of previous studies that have analyzed continental freshwater discharge. Listed in Table 2 are some of the previously published estimates of continental discharge based on observed streamflow (Shiklomanov 2003), model simulations of runoff (Nijssen et al. 2001), combinations of modeled runoff and observed streamflow (Fekete et al. 2000; 2002), and $P - E$ with the assumption of $\partial S/\partial t = 0$ (Baumgartner and Reichel 1975; Oki et al. 1995). Except for Fekete et al. (2000, 2002) and the current study, all the listed estimates are based on the consideration that the entire continent contributes to the freshwater discharged into the oceans. However, in contrast, and as mentioned earlier, large portions of

TABLE 1. Monthly mean, amplitude, and time of peak flow in the fitted seasonal cycles of freshwater discharge estimates from individual continents in km^3 $month^{-1}$.

Continent	GRACE–ECMWF	GRACE–NCEP–NCAR	Avg*	Amplitude**	Time of peak flow
Africa	209.6	393.1	302	178.7	Nov
Asia	648.7	661.5	619.3	639.2	Aug–Sep
Australasia	15.4	46.8	39.7	42	Feb
Europe	133.4	108.3	124.6	95.7	Feb
North America	500	591.6	538.9	69.8	Aug–Sep
South America	818.7	861	846.2	132.5	Apr

* The average is based on the average of GRACE–ECMWF and GRACE–NCEP–NCAR discharge estimates for the common period.
** Based on the seasonal cycles fitted to the average of GRACE–ECMWF and GRACE–NCEP–NCAR estimates of freshwater discharge over the common period.

TABLE 2. Comparison of mean annual freshwater discharge from individual continents in $km^3\ yr^{-1}$.

Source	Africa	Asia	Australasia	Europe	North America	South America
Observed						
Shiklomanov (2003)[a]	4047	13 510	2400/304	2900	7870	12 030
Modeled						
Nijssen et al. (2001)	3638	11 546	1715	2782	6209	10 210
Observed and modeled						
Fekete et al. (2000)	4263	13 046	712	2362	6381	11 621
Fekete et al. (2002)	4306	12 681	1320	2461	5883	11 663
$P - E$ ($\partial S/\partial t = 0$)						
Baumgartner and Reichel (1975)[b]	3400	12 200	2400/200	2800	5900	11 100
Oki et al. (1995)	−3006	10 476	480	1351	6379	7395
This study						
GRACE–ECMWF[c]	2515	7784	185	1601	6000	9828
GRACE–NCEP–NCAR[c]	4717	7938	561	1299	7104	10 332
Avg[c]	3624 ± 342	7432 ± 285	476 ± 121	1495 ± 166	6463 ± 264	10 154 ± 421

[a] The first estimate includes the whole of Australasia and the second estimate is for continental Australia based on gauged discharge (1921–85).

[b] The first estimate includes the whole of Australasia and the second estimate is just for the continent of Australia.

[c] Freshwater discharges estimated in this study from GRACE–ECMWF and GRACE–NCEP–NCAR in a land–atmosphere water balance and the average of the GRACE–ECMWF and GRACE–NCEP–NCAR discharge estimates over the common period are denoted by Avg.

continents such as Australasia, Asia, and Africa, are endorheic. Exclusion of endorheic regions can in part explain some of the noted differences among the cited discharge estimates (Table 2). Importantly, the majority of the inconsistencies noted in Table 2 are perhaps best explained by the much shorter time span used in the current study.

Even though our estimates are similar to those from the previous studies in Africa, North America, and South America, significant differences are noted in the discharge from Asia, Europe, and Australasia. The apparent high bias in discharge from Asia is the result of reduced net precipitation over the contributing drainage region during the study period. Conversion of the average of published discharges (~12 600 $km^3\ yr^{-1}$) from Asia, assuming $P - E$ to be equivalent of runoff at interannual time scales, yields a $P - E$ value of ~1050 $km^3\ month^{-1}$, whereas reanalysis-based $P - E$ values used in this study are ~670 (ECMWF) and ~687 $km^3\ month^{-1}$ (NCEP–NCAR). The estimated discharge from Europe is also the lowest among those listed but similar to the ECMWF-based estimate from Oki et al. (1995). Recently reported heat waves and subsequent precipitation deficits in Europe (Fischer et al. 2007) during the period of 2003–05 might be the primary cause behind the noted reduction in freshwater discharge from the region during the study period.

The Australasian drainage region is unique in the sense that the majority (85%) of this drainage region, occupied by continental Australia, produces negligible runoff compared to that observed from the whole region. In comparison to most previous studies, our estimate of freshwater discharge from this region (~476 $km^3\ yr^{-1}$) is the lowest. However, our estimates are quite comparable to those obtained from continental Australia only, for example, the second estimate of Shiklomanov (2003) and Baumgartner and Reichel (1975) in Table 2. Thus, we infer that runoff from the small islands and southern parts of New Guinea, which composes a major fraction of the freshwater discharge from the region, is mostly unaccounted for in our estimates. The primary reason for the noted inconsistency is that the current method does not have the ability to resolve discharge from islands such as those along the coast of Australia. This is because the current method is limited by a critical area ($>10^5\ km^2$) over which it can be effectively applied (Yeh et al. 1998; Seneviratne et al. 2004). More specifically, the $P - E$ estimates used in this study lack the spatial resolution to accurately quantify net precipitation over these regions. This limitation results in the encroachment of oceanic (large negative) $P - E$ patterns over the islands thereby resulting in negative or no discharge with the correction scheme used in this study. The GRACE data used in this study were also restricted by the spatial scale, primarily because of the smoothing procedure, over which the storage change signal can be detected with reasonable accuracy (Chen et al. 2005). Thus, we believe that freshwater discharges from islands such as those discussed above are probably best approximated from the climatologic gauge-based measurements. It is therefore necessary to include discharge from the islands in Australa-

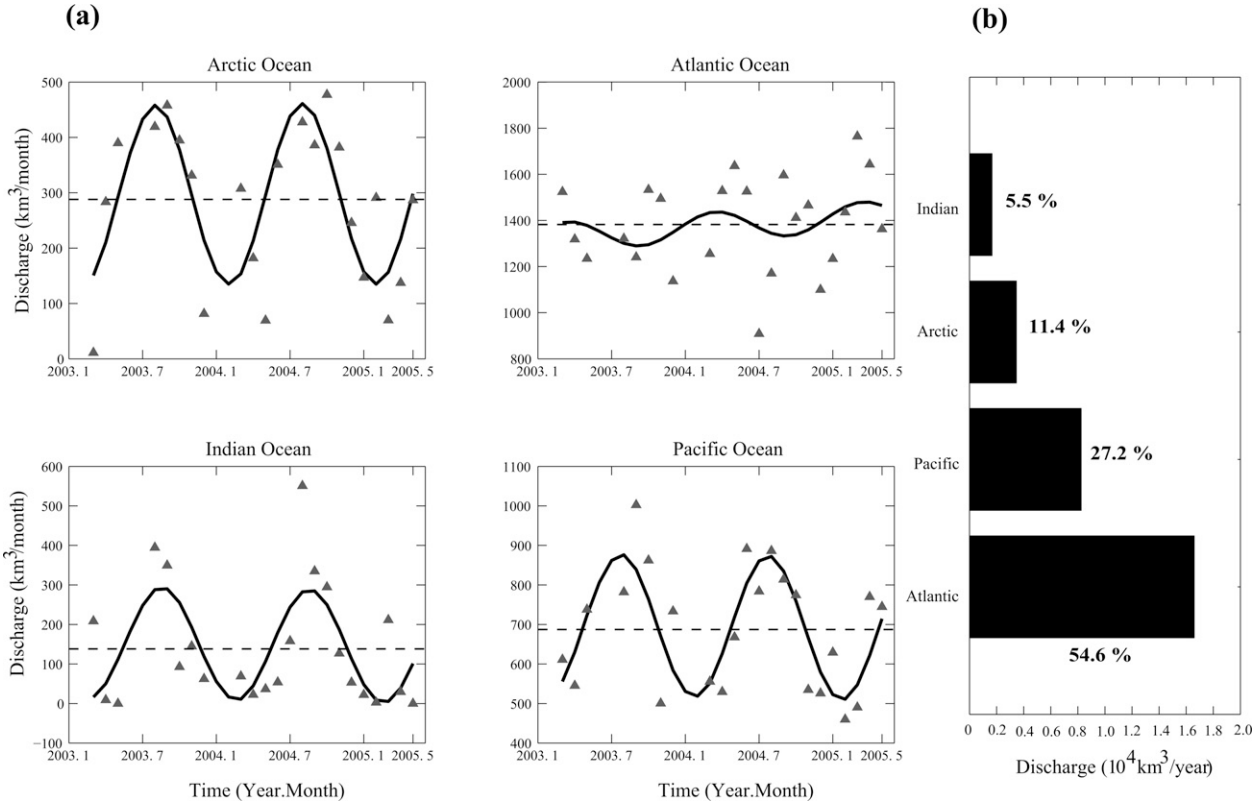

FIG. 4. (a) Monthly variations of freshwater discharge into individual oceans (triangles) and their fitted seasonal cycles (solid black line). The mean monthly discharge for the study is shown as broken black lines. (b) Relative contributions of freshwater discharge from each drainage region expressed as a percentage of the global discharge.

sia, deduced from previous studies, to put together a comprehensive quantification of global freshwater discharge using the current methodology (see section 8).

6. Discharge into world oceans

Monthly freshwater discharge is estimated for each of the drainage regions shown in Fig. 1b using the previously described method. Results shown in Fig. 4a are the average of the GRACE–ECMWF and GRACE–NCEP–NCAR discharge estimates for the common period. The triangles in Fig. 4a represent monthly values while the solid and dashed lines represent the fitted seasonal cycles and the mean monthly discharge for the study period. The amplitudes of the seasonal cycles of freshwater discharge into individual oceans, along with their monthly means, are shown in Table 3.

The mean monthly discharge into the Atlantic Ocean ($\sim$1382 km^3 month^{-1}) is the largest, while outflows into the Indian Ocean ($\sim$138 km^3 month^{-1}) are the least. Amplitudes of fitted seasonal cycles of discharge (based on a least squares fit) vary from a high of 181 km^3 month^{-1} for the Pacific Ocean to a low of 63 km^3 month^{-1} for the Atlantic Ocean (see Table 3 for details). Differences in the amplitude of variability are highlighted by the varying scales used in Fig. 4a. The timing of the peak discharge into the Atlantic Ocean (in March–April) is also distinctly different from those of the Arctic, Indian, and Pacific Oceans (in August).

While the large variance in monthly freshwater discharge into the Atlantic Ocean is similar to that observed in the estimates from North America (in Fig. 3a), the timing of the peak discharge (in March–April) is coincident with outflows from South America (Fig. 3a). Discharge into the Indian Ocean peaks around August as a result of large increases in river flow due to the Indian monsoons. Likewise, Pacific Ocean discharge shows a peak in August due to heavy precipitation from the Southeast Asian monsoons and is also reflected in the discharge estimates from river basins like the Mekong and Chang Jiang (Fig. 2). The seasonal cycle of discharge into the Arctic Ocean also has a high amplitude ($\sim$164 km^3 month^{-1}) with a peak in August, resulting from the late spring snowmelt, and a minimum in December–January due to extensive snowfall and

TABLE 3. Monthly mean, amplitude, and time of peak flow in the fitted seasonal cycles in freshwater discharges draining into individual ocean basins (km^3 $month^{-1}$).

Oceans	GRACE–ECMWF	GRACE–NCEP–NCAR	Avg*	Amplitude**	Time of peak flow
Arctic	290.1	304.6	287.9	163.8	Aug
Atlantic	1249.8	1508.9	1382.2	62.9	Mar–Apr
Indian	140.5	139	138.3	142	Aug
Pacific	665.7	756.7	687.1	181.3	Aug

* The average is based on the average of GRACE–ECMWF and GRACE–NCEP–NCAR discharges for the common period

** Based on the seasonal cycles fitted to the average of GRACE–ECMWF and GRACE–NCEP–NCAR estimates of freshwater discharge over the common period.

freezing of rivers. An evaluation of the relative amount of freshwater received by each of the oceans (Fig. 4b) reveals that the Atlantic Ocean receives the majority (~55%) of the global freshwater discharge, while the Indian Ocean receives the least (~5%). When viewed against a similar assessment made by Shiklomanov (2003), the relative percentages for the Atlantic, Pacific, and Arctic Oceans are extremely close even though their magnitudes differed slightly.

Comparisons of terrestrial freshwater discharge into the oceans, summarized in Table 4, show that our estimates compare very well with the majority of the previous studies, with the exception of the Indian Ocean. Only in the Arctic drainage region can we perform a direct comparison of the gauge-based discharge (McClelland et al. 2006) with our primarily observation-based estimates for the same time period (Syed et al. 2007). In brief, our estimated discharge was larger than that of McClelland et al. (2006), which is the most recent and comprehensive gauge-based observation of freshwater discharge. A similar direct comparison of discharge for the rest of the drainage regions is limited by the differences in the time periods over which annual averages were estimated by the previous studies.

However, in contrast to previous studies, our estimate for the Indian Ocean is significantly lower, most likely because our estimates only represent a very short period (3 yr) in the recent past. In contrast, all the previous studies aggregated individual streamflow observations for much longer periods spanning over various time intervals. A part of the noted differences can also be due to the exclusion of internally draining regions and because large arid and semiarid regions occupy significant portions of the contributing drainage area (e.g., Arabian Peninsula, coasts of eastern Africa and Australia). It should be noted here that arid and semiarid areas, such as those mentioned above, can actually yield values of E equal to P or even greater than P. Major irrigation and water storage projects, characteristic of these arid regions, can actually produce excess evapotranspiration and are duly represented in the $P - E$ estimates from the atmospheric moisture budget (Oki et al. 1995; Dai and Trenberth 2002) used in this study. On the contrary, current global land surface hy-

TABLE 4. Comparison of mean annual freshwater discharge into individual ocean basins (km^3 yr^{-1}).

Source	Arctic	Atlantic	Indian	Pacific
Observed				
Shiklomanov (2003)	4280	20 190	4530	10 530
Observed and modeled				
Fekete et al. (2000)	2947	18 357	4802	11 127
Dai and Trenberth (2002)	3658	19 168	4532	9092
Fekete et al. (2002)	3268	18 507	4858	10 476
$P - E$ ($\partial S/\partial t = 0$)				
Baumgartner and Reichel (1975)	2600	19 300	5600	12 200
Oki (1999)	4500	21 500	4000	10 000
This study				
GRACE–ECMWF*	3482	14 998	1686	7988
GRACE–NCEP–NCAR*	3654	18 107	1668	9080
Avg*	3455 ± 363	16 586 ± 510	1660 ± 300	8245 ± 184

* Freshwater discharges estimated in this study from GRACE–ECMWF and GRACE–NCEP–NCAR in a land–atmosphere water balance and the average of GRACE–ECMWF and GRACE–NCEP–NCAR discharge estimates over the common period are denoted by Avg.

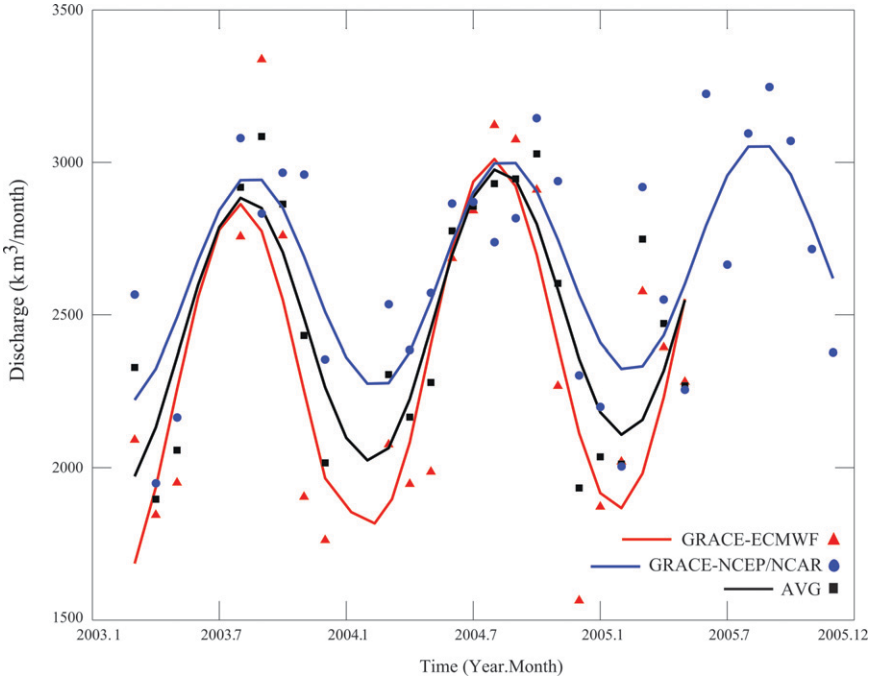

FIG. 5. Monthly variations of global freshwater discharge from GRACE–ECMWF (red triangles), GRACE–NCEP–NCAR (blue circles), and their average over the common period (black squares). The seasonal cycles fitted (solid lines) to the monthly estimates are shown in their respective colors.

drologic models are still incapable of accounting for these excess evaporative losses. As a result, our approach produces less discharge compared to those based on model simulations. In addition, these large-scale discharge estimates based on streamflow data observed over varying periods from the early twentieth century do not reflect on the impacts of widespread regulations imposed on most surface water bodies (Vörosmarty et al. 2000b; Gleick 2003).

7. Global freshwater discharge

Shown in Fig. 5 are monthly estimates of global freshwater discharge excluding Greenland and Antarctica. Results shown are the monthly values (symbols) of discharge obtained from GRACE–ECMWF (red), GRACE–NCEP–NCAR (blue), and the average of the two (black) over the common period. Seasonal cycles (solid lines) fitted to each of the monthly estimates are represented in their respective colors. For the study period we estimate global freshwater discharge rates of 28 590 ± 1685 $km^3\ yr^{-1}$ (GRACE–ECMWF), 32 851 ± 744 $km^3\ yr^{-1}$ (GRACE–NCEP–NCAR), and 30 354 ± 212 $km^3\ yr^{-1}$ (using the average of GRACE–ECMWF and GRACE–NCEP–NCAR estimates over the common period). The amplitude of the seasonal cycles of global discharge from GRACE–NCEP–NCAR (~750 $km^3\ month^{-1}$) is smaller than that computed from GRACE–ECMWF (~950 $km^3\ month^{-1}$). While the maxima of discharge from GRACE–ECMWF and GRACE–NCEP–NCAR are similar in magnitude, the minima in these estimates are distinctly different. Low flows in GRACE–NCEP–NCAR discharge estimates are consistently higher than those of GRACE–ECMWF. Globally, terrestrial freshwater discharge peaks during August–September and reaches a minimum in February, consistent with the high precipitation over the Northern Hemisphere tropics due to the seasonal migration of the ITCZ.

Listed in Table 5 are some of the previously reported global freshwater discharge estimates and the methods used in the computation. Our estimates of global terrestrial discharge are in general lower than most prior estimates, which is due to a number of different factors. For example, unlike most of the previous studies, which presented long-term annual averages, the current estimates are based on a short-term average over the period of 2003–05. The length of the discharge dataset used can significantly affect the annual mean values, depending on the inclusion and exclusion of wet and dry years. According to Gleick (2003), Shiklomanov (2003), and Nilsson et al. (2005), in all likelihood, dis-

TABLE 5. Comparison of mean annual global freshwater discharge ($km^3\ yr^{-1}$).

Source	Methodology	Discharge
Baumgartner and Reichel (1975)	Gauge-based precipitation minus modeled evapotranspiration with $\partial S/\partial t = 0$	37 713
Oki et al. (1995)	ECMWF (1985–88): atmospheric budget analysis with $\partial S/\partial t = 0$	22 311
Perry et al. (1996)	Scaled from 981 river basin discharges	37 743
Oki (1999)	ECMWF (1989–92): atmospheric budget analysis with $\partial S/\partial t = 0$	40 000
Fekete et al. (2000)	Water balance model simulation constrained by observed streamflow	38 402
Nijssen et al. (2001)	Hydrologic model output	36 103
Dai and Trenberth (2002)	Scaled from 921 largest river basin discharges supplemented by modeled runoff	37 288 ± 662
Fekete et al. (2002)	Water balance model output constrained by observed streamflow	38 314
Schlosser and Houser (2007)	Climate Prediction Center Merged Analysis of Precipitation–Global Precipitation Climatology Project (CMAP–GPCP) precipitation minus modeled evapotranspiration with $\partial S/\partial t = 0$	?36 000
GRACE–ECMWF*	GRACE–ECMWF in land–atmosphere water balance	28 590 ± 1685
GRACE–NCEP–NCAR*	GRACE–NCEP–NCAR in land–atmosphere water balance	32 851 ± 1744
Avg*	Average of ECMWF and NCEP–NCAR	30 354 ± 1212

* Freshwater discharges estimated in this study from GRACE–ECMWF and GRACE–NCEP–NCAR in a land–atmosphere water balance and the average of GRACE–ECMWF and GRACE–NCEP–NCAR discharge estimates over the common period are denoted by Avg.

charge in the modern era has changed drastically from that earlier in the record, due to large-scale changes in land use, reservoir storage, and consumption–management practices, particularly in Africa, Asia, and South America. The noted differences can also be attributed to the exclusion of contributions from large endorheic regions, consideration of $\partial S/\partial t \neq 0$, and also due to the lack of spatial resolve in the current method to identify contributions from the Pacific islands in Australasia.

Figure 6 shows the mean annual freshwater discharge (average of GRACE–ECMWF and GRACE–NCEP–NCAR) from land by 10° latitudinal zones. The most distinctive feature in the uneven distribution of flows into the World Ocean is its bimodality. The greater volume of discharge in the Northern Hemisphere is due to the greater percentage of land. The distribution peaks in the equatorial belt followed by a secondary maximum at 63°–53°N, reflecting the global distribution of precipitation. Nearly 43% of the mean annual discharge enters the World Ocean between the latitudes 13°N and 6°S predominantly due to contributions from the several of the world's largest river basins (e.g., Amazon, Orinoco, Congo, and Niger). Similarly, the Northern Hemisphere peak is due to inputs from some of the largest Eurasian (e.g., Ob, Lena, and Yenisei) and North American (e.g., Mackenzie and Yukon) rivers flowing into the Arctic Ocean. While the zonal distribution pattern of our freshwater discharge is very similar to that demonstrated in Shiklomanov (2003), the actual magnitudes are quite different, particularly in the Northern Hemisphere tropics.

8. Closure of the global freshwater budget

Global freshwater discharge can also be computed as input to a global ocean mass balance. Discharge computed in this manner, R_o, can be compared to that computed as discharge from the continents (global R_l). The difference between R_o [see Eq. (8) below] and global R_l [Eq. (6)] is one measure of global water budget closure. The global freshwater budget for the oceans can be represented as follows:

$$\frac{\partial M_o}{\partial t} = -\left(\frac{\partial W}{\partial t}\right)_o - (\nabla \cdot \mathbf{Q})_o + R_o, \tag{7}$$

where $\partial M_o/\partial t$ represents the time derivative of ocean mass variations observed by GRACE (Chambers et al. 2004); $(\partial W/\partial t)_o$ and $(\nabla \cdot \mathbf{Q})_o$ represent the column-integrated precipitable water tendency and horizontal divergence of the vertically integrated moisture flux over the global ocean surface (obtained from ECMWF and NCEP–NCAR reanalysis datasets), respectively; and R_o represents freshwater discharged into the global oceans. Rearranging Eq. (7),

$$R_o = \left(\frac{\partial W}{\partial t}\right)_o + (\nabla \cdot \mathbf{Q})_o + \frac{\partial M_o}{\partial t}. \tag{8}$$

Monthly values of global freshwater discharge (R_o and global R_l) for the study period are shown in Fig. 7a

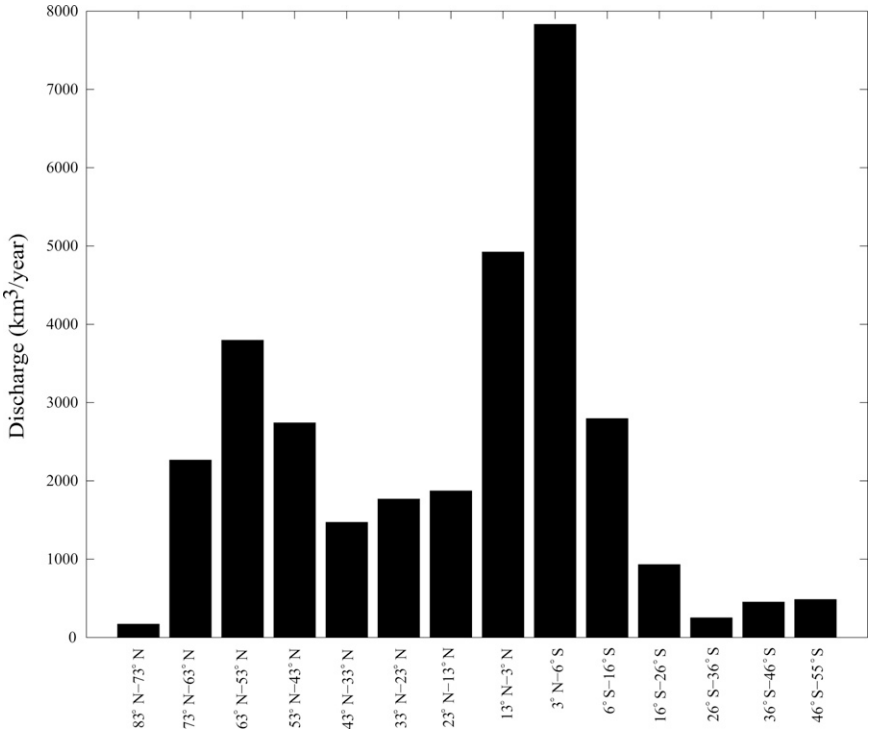

FIG. 6. Zonal variation of mean annual freshwater discharge based on the average of GRACE–ECMWF and GRACE–NCEP–NCAR discharge estimates.

and the seasonal cycles fitted to these monthly values are shown in Fig. 7b. Results shown in Figs. 7a and 7b are the averages of the GRACE–ECMWF and GRACE–NCEP–NCAR discharge estimates for the common period. The corresponding differences between R_o and global R_l, at monthly and seasonal time scales, are shown in Figs. 7c and 7d, respectively. The means of the differences at monthly (Fig. 7c) and seasonal time scales (Fig. 7d), shown as thick broken lines, are nearly equal to zero. The close agreement between the two estimates at monthly (RMSE = 329 km^3 month^{-1}) and seasonal (RMSE = 147 km^3 month^{-1}) time scales is encouraging in the context of global water budget closure.

Because our estimate of R_o includes a mass change term for the global ocean as directly measured by GRACE, it implicitly includes melt contributions from the Greenland and Antarctic ice sheets. In contrast, our estimates of continental freshwater discharge exclude contributions from the ice sheets and islands in Australasia. Based on the oceanic freshwater budget, the computed global freshwater discharge is 27 212 ± 1450 km^3 yr^{-1} (GRACE–ECMWF) and 34 063 ± 1540 km^3 yr^{-1} (GRACE–NCEP–NCAR). The average of the two estimates for the common period is 30 280 ± 1495 km^3 yr^{-1}. To present a comprehensive depiction of global freshwater discharge, contributions from other land sources are added to both R_o and global R_l (Table 6).

Ramillien et al. (2006b), Velicogna and Wahr (2006a, b), Chen et al. (2006b), and Luthcke et al. (2006) presented the most recent quantification of ice mass losses from Greenland and Antarctica. However, the estimates provided by Velicogna and Wahr (2006a, b) and Ramillien et al. (2006b) define the range in the combined ice mass loses from Greenland and Antarctica, the average of which is ~284 km^3 yr^{-1}. Addition of the ice-sheet mass losses and discharge from the islands in Australasia (2048 km^3 yr^{-1}) to that of the freshwater discharge obtained from the terrestrial water balance (global R_l) yields an estimate of 32 686 km^3 yr^{-1}. Similarly, freshwater discharge estimates obtained as an input into global oceans (R_o), when combined with contributions from the islands in Australasia, bring the global freshwater discharge to 32 328 km^3 yr^{-1}. The difference between R_o and global R_l is 358 km^3 yr^{-1}, indicating closure at the 1% level. The close agreement between R_o and global R_l is an important measure of the water balance closure and provides an independent assessment of the validity of the method used here.

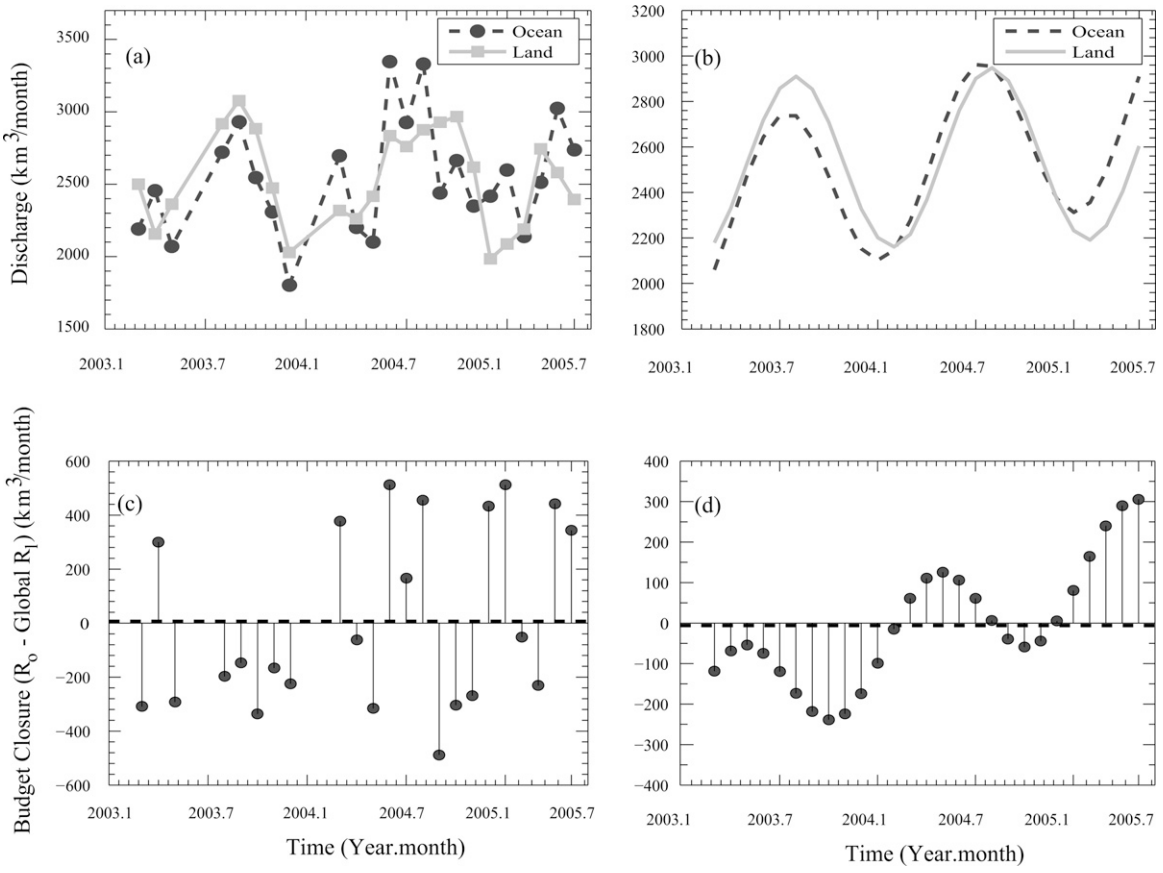

FIG. 7. (a) Month-to-month variation of global freshwater discharge computed as input to global ocean mass balance (R_o) and those estimated using water balance over global land (global R_l). (b) Monthly variation of the seasonal cycles fitted to monthly estimates of R_o and global R_l. (c) Differences in the monthly values of R_o and global R_l. (d) Differences in the fitted seasonal cycles of R_o and global R_l.

9. Summary and conclusions

In this study we have presented new estimates of terrestrial freshwater discharge from basin to continental scales. The method is based on the synergistic use of GRACE terrestrial water storage change estimates with ECMWF and NCEP–NCAR reanalysis data in a combined land–atmosphere water balance. Previous applications of the coupled land–atmosphere water balance to discharge estimation required the assumption that $\partial S/\partial t$ in (6) equals zero. The availability of monthly GRACE-based terrestrial water storage changes allows us to relax this assumption and, for the first time, to calculate contemporary, large-scale freshwater discharge estimates at monthly intervals. Implicit in our mass balance–based estimates are the influence of water mass losses due to water management and land-use changes, as well as discharge from ungauged portions of the contributing drainage area and direct groundwater discharge. While the use of ECMWF and NCEP–NCAR data in the computation of freshwater discharges defines the range in the values, the average of the two provides a more robust estimate by eliminating the individual biases.

TABLE 6. Assessment of global water budget closure.

Source	Estimate ($km^3\ yr^{-1}$)
Terrestrial outflows	
Global R_l (this study)	30 354 ± 1212
Ice sheets* (Velicogna and Wahr 2006a,b)	400 ± 88
Ice sheets* (Ramillien et al. 2006b)	169 ± 30
Avg of ice sheets	284 ± 59
Islands in Australasia (Shiklomanov 2003)	2048 ± 205
Total terrestrial outflow	32 686 ± 1727
Ocean inflows	
R_o (this study)	30 280 ± 1495
Islands in Australasia (Shiklomanov 2003)	2048 ± 205
Total ocean inflow	32 328 ± 1513
Closure (total terrestrial outflow–total ocean inflow)	358

* Includes Greenland and Antarctica.

Annual cycles of the observed streamflow were compared with those of the computed discharge and $P - E$

in some of the world's largest river basins. Results showed very good agreement between the observed and estimated discharges ($R = 0.77$) while highlighting the importance of storage changes in estimating discharge using a water balance approach.

Freshwater discharge from South America (~846 km^3 month^{-1}) was the largest among that estimated from the continents while flows into the Atlantic Ocean (~1382 km^3 month^{-1}) were the largest among the drainage regions, accounting for 34% and 55% of global discharge, respectively. The amplitudes of fitted seasonal cycles varied between 639.2 km^3 month^{-1}(Asia) and 42 km^3 month^{-1}(Australasia) among the continents and between 181 km^3 month^{-1} (Pacific Ocean) and 63 km^3 month^{-1} (Atlantic Ocean) among the drainage regions.

Our estimate of the global discharge for the period of 2003–05, using the average of GRACE–ECMWF and GRACE–NCEP–NCAR discharge estimates over the common period, is 30 354 ± 1212 km^3 yr^{-1}. Monthly variations of global freshwater discharge peak between August and September and reach a minimum in February. While the peaks in global discharge differed little in magnitude, the minima in GRACE–ECMWF discharge estimates were significantly smaller than those for the GRACE–NCEP–NCAR discharge. The zonal distribution of freshwater discharge from land revealed a bimodality with its primary peak between 13°S and 6°N and a secondary peak between 63° and 53°N, which corresponds to the global distribution of precipitation.

Results from this study were comparable to previous gauge-based observations, in particular considering a 10%–20% uncertainty in most stream gauge data (Fekete et al. 2002). When placed within the context of previous studies, the current estimates agreed reasonably well, except for flows from Asia and those into the Indian Ocean. The noted inconsistencies are perhaps best explained by the fundamental difference in the two estimates, the current estimate being a more holistic representation of freshwater outflow in comparison to observed streamflow, and also due to the exclusion of contributions from endorheic regions, consideration of nonzero storage change in (6), and that the current estimates were short-term averages over the period of 2003–05.

To provide an independent check on the terrestrial water balance–based estimates and as a measure of global water budget closure, the global freshwater discharge was also computed as inflow in the global ocean mass balance. The proximity of these two estimates, both in terms of their annual (358 km^3 yr^{-1}) and monthly (RMSE = 329 km^3 month^{-1}) discharges, shows promise for the monitoring of large-scale freshwater discharge using the method presented here. Notwithstanding the differences, our method provides monthly time series of gauge-independent, large-scale freshwater discharge estimates, complementary to those currently available, and to those that may ultimately be derived from a dedicated surface water altimetry mission.

Acknowledgments. This research was sponsored by NASA IDS Grant NNG04G092G and NASA Earth and Space Science Fellowship funding (NNG05GP43H). This support is gratefully acknowledged.

REFERENCES

Alsdorf, D. E., and D. P. Lettenmaier, 2003: Tracking fresh water from space. *Science,* **301,** 1491–1494.

——, E. Rodríguez, and D. P. Lettenmaier, 2007: Measuring surface water from space. *Rev. Geophys.,* **45,** RG2002, doi:10.1028/2006RG000197.

Baumgartner, A., and E. Reichel, 1975: *The World Water Balance.* Elsevier, 179 pp.

Betts, A. K., J. H. Ball, P. Viterbo, A. Dai, and J. Marengo, 2005: Hydrometeorology of the Amazon in ERA-40. *J. Hydrometeor.,* **6,** 764–773.

Bjerklie, D. M., S. L. Dingman, C. J. Vörösmarty, C. H. Bolster, and R. G. Congalton, 2003: Evaluating the potential for measuring river discharge from space. *J. Hydrol.,* **278,** 17–38.

Brakenridge, G. R., S. V. Nghiem, E. Anderson, and S. Chien, 2005: Space-based measurement of river runoff. *Eos, Trans. Amer. Geophys. Union,* **86,** 185–188.

Branstetter, M. L., 2001: Development of a parallel river transport algorithm and applications to climate studies. Ph.D. dissertation, University of Texas at Austin, 119 pp.

Chambers, D. P., 2006: Evaluation of new GRACE time-variable gravity data over the ocean. *Geophys. Res. Lett.,* **33,** L17603, doi:10.1029/2006GL027296.

——, J. Wahr, and R. S. Nerem, 2004: Preliminary observations of global ocean mass variations with GRACE. *Geophys. Res. Lett.,* **31,** L13310, doi:10.1029/2004GL020461.

Chen, J. L., C. R. Wilson, J. S. Famiglietti, and M. Rodell, 2005: Spatial sensitivity of the Gravity Recovery and Climate Experiment (GRACE) time-variable gravity observations. *J. Geophys. Res.,* **110,** B08408, doi:10.1029/2004JB003536.

——, ——, ——, and ——, 2006a: Attenuation effect on seasonal basin-scale water storage changes from GRACE time-variable gravity. *J. Geodesy,* **81** (4), 237–245, doi:10.1007/s00190-006-0104-2.

——, ——, and B. D. Tapley, 2006b: Satellite gravity measurements confirm accelerated melting of Greenland ice sheet. *Science,* **313,** 1958–1960.

Coe, M. T., 2000: Modeling terrestrial hydrologic systems at the continental scale: Testing the accuracy of an atmospheric GCM. *J. Climate,* **13,** 686–704.

Cullather, R. I., D. H. Bromwich, and M. C. Serreze, 2000: The atmospheric hydrologic cycle over the Arctic basin from reanalyses. Part I: Comparison with observations and previous studies. *J. Climate,* **13,** 923–937.

Dai, A., and K. E. Trenberth, 2002: Estimates of freshwater discharge from continents: Latitudinal and seasonal variations. *J. Hydrometeor.,* **3,** 660–687.

Fekete, B. M., C. J. Vörösmarty, and W. Grabs, 2000: Global composite runoff fields based on observed data and simulated water balance. Global Runoff Data Centre Tech. Rep. 22, Koblenz, Germany, 108 pp. [Available online at http://www.bafg.de/grdc.htm.]

——, ——, and ——, 2002: High-resolution fields of global runoff combining observed river discharge and simulated water balances. *Global Biogeochem. Cycles,* **16,** 1042, doi:10.1029/1999GB001254.

Fischer, E. M., S. I. Seneviratne, D. Lüthi, and C. Schär, 2007: Contribution of land–atmosphere coupling to recent European summer heat waves. *Geophys. Res. Lett.,* **34,** L06707, doi:10.1029/2006GL029068.

Frappart, F., G. Ramillien, S. Biancamaria, N. M. Mognard, and A. Cazenave, 2006: Evolution of high-latitude snow mass derived from the GRACE gravimetry mission (2002–2004). *Geophys. Res. Lett.,* **33,** L02501, doi:10.1029/2005GL024778.

Gleick, P. H., 2003: Global freshwater resources: Soft-path solutions for the 21st century. *Science,* **302,** 1524–1528, doi:10.1126/science.1089967.

Gutowski, W. J. J., Y. Chen, and Z. Ötles, 1997: Atmospheric water vapor transport in NCEP–NCAR reanalyses: Comparison with river discharge in the central United States. *Bull. Amer. Meteor. Soc.,* **78,** 1957–1969.

Haddeland, I., T. Skaugen, and D. P. Lettenmaier, 2006: Anthropogenic impacts on continental surface water fluxes. *Geophys. Res. Lett.,* **33,** L08406, doi:10.1029/2006GL026047.

Han, S. C., C. K. Shum, C. Jekeli, C. Y. Kuo, C. Wilson, and K. W. Seo, 2005: Nonisotropic filtering of GRACE temporal gravity for geophysical signal enhancement. *Geophys. J. Int.,* **163,** 18–25, doi:10.1111/j.1365-246X.2005.02756.

Kalnay, E., and Coauthors, 1996: The NCEP–NCAR 40-Year Reanalysis Project. *Bull. Amer. Meteor. Soc.,* **77,** 437–471.

Lohmann, D., and Coauthors, 2004: Streamflow and water balance intercomparisons of four land surface models in the North American Land Data Assimilation System project. *J. Geophys. Res.,* **109,** D07S91, doi:10.1029/2003JD003517.

Luthcke, S. B., and Coauthors, 2006: Recent Greenland ice mass loss by drainage system from satellite gravity observations. *Science,* **314,** 1286–1289.

McClelland, J. W., S. J. Déry, B. J. Peterson, R. M. Holmes, and E. F. Wood, 2006: A pan-Arctic evaluation of changes in river discharge during the latter half of the 20th century. *Geophys. Res. Lett.,* **33,** L06715, doi:10.1029/2006GL025753.

Nijssen, B., G. M. O'Donnell, D. P. Lettenmaier, D. Lohmann, and E. F. Wood, 2001: Predicting the discharge of global rivers. *J. Climate,* **14,** 3307–3323.

Nilsson, C., C. A. Reidy, M. Dynesius, and C. Revenga, 2005: Fragmentation and flow regulation of the world's large river systems. *Science,* **308,** 405–408, doi:10.1126/science.1107887.

Niu, G.-Y., and Z.-L. Yang, 2006: Assessing a land surface model's improvements with GRACE estimates. *Geophys. Res. Lett.,* **33,** L07401, doi:10.1029/2005GL025555.

NRC, 2007: *Earth Science and Applications from Space: National Imperatives for the Next Decade and Beyond*. National Academies Press, 428 pp.

Oki, T., 1999: The global water cycle. *Global Energy and Water Cycles,* K. A. Browning and R. J. Gurney, Eds., Cambridge University Press, 10–29.

——, K. Musiake, H. Matsuyama, and K. Masuda, 1995: Global atmospheric water balance and runoff from large river basins. *Hydrol. Processes,* **9,** 655–678.

Peixóto, J. P., and A. H. Oort, 1992: *Physics of Climate.* AIP Press, 520 pp.

Perry, G. D., P. B. Duffy, and N. L. Miller, 1996: An extended data set of river discharges for validation of general circulation models. *J. Geophys. Res.,* **101** (D16), 21 339–21 349.

Prigent, C., E. Matthews, F. Aires, and W. B. Rossow, 2001: Remote sensing of global wetland dynamics with multiple satellite data sets. *Geophys. Res. Lett.,* **28,** 4631–4634.

Probst, J. L., and Y. Tardy, 1987: Long range streamflow and world continental runoff fluctuations since the beginning of the century. *J. Hydrol.,* **94,** 289–311.

Ramillien, G., F. Frappart, A. Cazenave, and A. Guntner, 2005: Time variations of land water storage from an inversion of 2 years of GRACE geoids. *Earth Planet. Sci. Lett.,* **235,** 283–301.

——, ——, A. Güntner, T. Ngo-Duc, A. Cazenave, and K. Laval, 2006a: Time variations of the regional evapotranspiration rate from Gravity Recovery and Climate Experiment (GRACE) satellite gravimetry. *Water Resour. Res.,* **42,** W10403, doi:10.1029/2005WR004331.

——, A. Lombard, A. Cazenave, E. R. Ivins, M. Llubes, F. Remy, and R. Biancale, 2006b: Interannual variations of the mass balance of the Antarctica and Greenland ice sheets from GRACE. *Global Planet. Change,* **53,** 198–208, doi:10.1016/j.gloplacha.2006.06.003.

Roads, J., and A. Betts, 2000: NCEP–NCAR and ECMWF reanalysis surface water and energy budgets for the Mississippi River basin. *J. Hydrometeor.,* **1,** 88–94.

——, and Coauthors, 2003: GCIP water and energy budget synthesis (WEBS). *J. Geophys. Res.,* **108,** 8609, doi:10.1029/2002JD002583.

Rodda, J. C., S. A. Pieyns, N. S. Sehmi, and G. Matthews, 1993: Towards a world hydrological cycle observing system. *Hydrol. Sci. J.,* **38,** 373–378.

Rodell, M., and J. S. Famiglietti, 1999: Detectability of variations in continental water storage from satellite observations of the time dependent gravity field. *Water Resour. Res.,* **35,** 2705–2723.

——, ——, J. Chen, S. I. Seneviratne, P. Viterbo, S. Holl, and C. R. Wilson, 2004: Basin scale estimates of evapotranspiration using GRACE and other observations. *Geophys. Res. Lett.,* **31,** L20504, doi:10.1029/2004GL020873.

——, J. Chen, H. Kato, J. S. Famiglietti, J. Nigro, and C. R. Wilson, 2007: Estimating groundwater storage changes in the Mississippi River basin (USA) using GRACE. *Hydrogeol. J.,* **15,** 159–166.

Rowlands, D. D., S. B. Luthcke, S. M. Lkosko, F. G. R. Lemoine, D. S. Chinn, J. J. McCarthy, C. M. Cox, and O. B. Andersen, 2005: Resolving mass flux at high spatial and temporal resolution using GRACE satellite measurements. *Geophys. Res. Lett.,* **32,** L04310, doi:10.1029/2004GL021908.

Schlosser, C. A., and P. R. Houser, 2007: Assessing a satellite-era perspective of the global water cycle. *J. Climate,* **20,** 1316–1338.

Schmidt, R., and Coauthors, 2006: GRACE observations of changes in continental water storage. *Global Planet. Change,* **50,** 112–126.

Seneviratne, S. I., P. Viterbo, D. Luthi, and C. Schar, 2004: Inferring changes in terrestrial water storage using ERA-40 reanalysis data: The Mississippi River basin. *J. Climate,* **17,** 2039–2057.

Seo, K.-W., and C. R. Wilson, 2005: Simulated estimation of hydrological loads from GRACE. *J. Geodesy,* **78,** 442–456.

——, ——, J. S. Famiglietti, J. L. Chen, and M. Rodell, 2006: Terrestrial water mass load changes from Gravity Recovery and Climate Experiment (GRACE). *Water Resour. Res.,* **42,** 5417, doi:10.1029/2005WR004255.

Shiklomanov, I. A., 2003: Global renewable water resources in space and time. *World Water Resources at the Beginning of the Twenty-First Century,* I. A. Shiklomanov and J. C. Rodda, Eds., International Hydrology Series, Cambridge University Press, 352–368.

——, R. B. Lammers, and C. J. Vörösmarty, 2002: Widespread decline in hydrological monitoring threatens pan-Arctic research. *Eos, Trans. Amer. Geophys. Union,* **83,** 13–16.

Stokstad, E., 1999: Scarcity of rain, stream gages threatens forecasts. *Science,* **285,** 1199–1200, doi:10.1126/science.285.5431.1199.

Swenson, S. C., and P. C. D. Milly, 2006: Climate model biases in seasonality of continental water storage revealed by satellite gravimetry. *Water Resour. Res.,* **42,** W03201, doi:10.1029/2005WRR004628.

——, and J. Wahr, 2006a: Estimating large-scale precipitation minus evaporation from GRACE satellite gravity measurements. *J. Hydrometeor.,* **7,** 252–270.

——, and ——, 2006b: Post-processing removal of correlated errors in GRACE data. *Geophys. Res. Lett.,* **33,** L08402, doi:10.1029/2005GL025285.

——, ——, and P. C. D. Milly, 2003: Estimated accuracies of regional water storage variations inferred from the Gravity Recovery and Climate Experiment (GRACE). *Water Resour. Res.,* **39,** 1223, doi:10.1029/2002WR001808.

——, P. J.-F. Yeh, J. Wahr, and J. Famiglietti, 2006: A comparison of terrestrial water storage variations from GRACE with in situ measurements from Illinois. *Geophys. Res. Lett.,* **33,** L16401, doi:10.1029/2006GL026962.

——, J. Famiglietti, J. B. Basara, and J. M. Wahr, 2007: Estimating profile soil moisture and groundwater variations using GRACE and Oklahoma mesonet soil moisture data. *Water Resour. Res.,* **44,** W01413, doi:10.1029/2007WR006057.

Syed, T. H., J. S. Famiglietti, J. Chen, M. Rodell, S. I. Seneviratne, P. Viterbo, and C. R. Wilson, 2005: Total basin discharge for the Amazon and Mississippi River basins from GRACE and a land–atmosphere water balance. *Geophys. Res. Lett.,* **32,** L24404, doi:10.1029/2005GL024851.

——, ——, V. Zlotnicki, and M. Rodell, 2007: Contemporary estimates of Arctic freshwater discharge from GRACE and reanalysis. *Geophys. Res. Lett.,* **34,** L19404, doi:10.1029/2007GL031254.

——, ——, M. Rodell, J. Chen, and C. R. Wilson, 2008: Analysis of terrestrial water storage changes from GRACE and GLDAS. *Water Resour. Res.,* **44,** W02433, doi:10.1029/2006WR005779.

Tapley, B. D., S. Bettadpur, J. C. Ries, P. F. Thompson, and M. M. Watkins, 2004: GRACE measurements of mass variability in the earth system. *Science,* **305,** 503–505.

Trenberth, K. E., and C. J. Guillemot, 1998: Evaluation of the atmospheric moisture and hydrological cycle in the NCEP–NCAR reanalyses. *Climate Dyn.,* **14,** 213–231.

——, L. Smith, T. Qian, A. Dai, and J. Fasullo, 2007: Estimates of the global water budget and its annual cycle using observational and model data. *J. Hydrometeor.,* **8,** 754–769.

Velicogna, I., and J. Wahr, 2006a: Acceleration of Greenland ice mass loss in spring 2004. *Nature,* **443,** 329–331.

——, and ——, 2006b: Measurements of time-variable gravity show mass loss in Antarctica. *Science,* **311,** 1754–1756.

Vörösmarty, C. J., B. M. Fekete, M. Meybeck, and R. B. Lammers, 2000a: Global system of rivers: Its role in organizing continental land mass and defining land-to-ocean linkages. *Global Biogeochem. Cycles,* **14,** 599–621.

——, P. Green, J. Salisbury, and R. B. Lammers, 2000b: Global water resources: Vulnerability from climate change and population growth. *Science,* **289,** 284–288.

Wahr, J., M. Molenaar, and F. Bryan, 1998: Time variability of the Earth's gravity field: Hydrological and oceanic effects and their possible detection using GRACE. *J. Geophys. Res.,* **103** (B12), 30 205–30 229.

——, S. Swenson, V. Zlotnicki, and I. Velicogna, 2004: Time-variable gravity from GRACE: First results. *Geophys. Res. Lett.,* **31,** L11501, doi:10.1029/2004GL019779.

——, ——, and I. Velicogna, 2006: Accuracy of GRACE mass estimates. *Geophys. Res. Lett.,* **33,** L06401, doi:10.1029/2005GL025305.

Yeh, P. J.-F., M. Irizarry, and E. A. B. Eltahir, 1998: Hydroclimatology of Illinois: A comparison of monthly evaporation estimates based on atmospheric water balance and soil water balance. *J. Geophys. Res.,* **103** (D16), 19 823–19 837.

——, S. C. Swenson, J. S. Famiglietti, and J. Wahr, 2006: Remote sensing of groundwater storage changes in Illinois using the Gravity Recovery and Climate Experiment (GRACE). *Water Resour. Res.,* **42,** W12203, doi:10.1029/2006WR005374.

Zektser, I. S., and H. A. Loaiciga, 1993: Groundwater fluxes in the global hydrologic cycle: Past, present and future. *J. Hydrol.,* **144,** 405–427.